In vivo imaging using X-ray phase-contrast microtomography

Julian Moosmann

August 17, 2015, Philips Hamburg

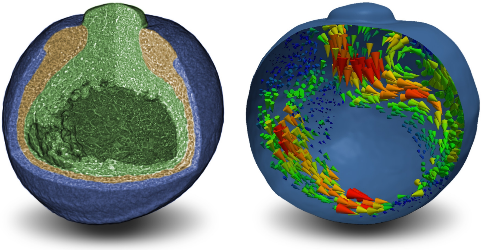

Outline

Introduction & Motivation

Experimental setup & principles of propagation-based phase contrast

Phase retrieval

In vivo imaging

Introduction

- Hard X-rays are strongly penetrating electromagnetic waves
- Interaction of X-ray and matter described by refractive index

$$n = 1 - \delta + i\beta$$

- Absorption: $\sqrt{I_0} = \frac{2\pi}{\lambda} \int dz \, \beta(z)$
  Phase: $\phi_0 = \frac{2\pi}{\lambda} \int dz \, \delta(z)$
- Use monochromatic coherent X-ray with energies s.t.

$$\delta / \beta \gg 1$$

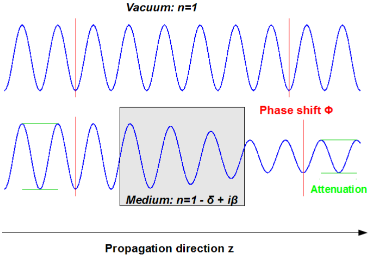

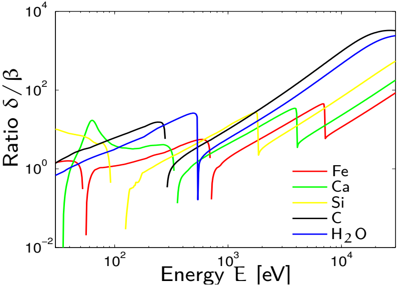

➡ Imaging of weakly absorbing materials using phase-contrast

Motivation

- Biological specimen w/o cartilage, bone, & blood vessels are essentially pure-phase objects for $E > 20\,\mathrm{keV}$
- Imaging techniques to study the development of model organisms are essential tools in Biology, Medicine, Toxicology, ...
- Examples of important vertebrate model organisms


Xenopus laevis

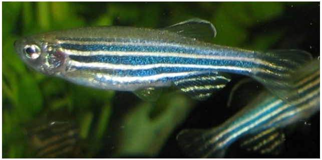
zebrafish


lamprey

Comparison: 4D imaging techniques

- Optical microscopy
  - Non-destructive: Surfaces / thin samples
  - Destructive: Sectioning
- Fluorescence microscopy
  - Expression of fluorescence marker
  - Photobleaching
  - Sparse information
  - Limited depth information: few cell layers
- Magnetic Resonance Imaging
  - Non-destructive
  - Dense & deep information
  - Limited spatial & temporal resolution

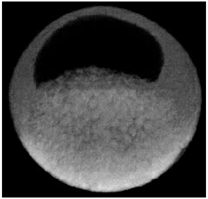

Xenopus: optical, sectioned

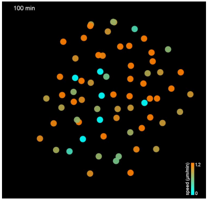

Zebrafish: light-sheet microscopy

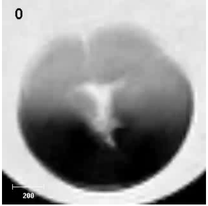

Xenopus: MRI

Comparison: 4D imaging techniques

- X-ray phase-contrast tomography
  - Fast
  - Dense 3D information
  - Apt for optically opaque objects
  - Possible time lapse $\lesssim 2\,\mathrm{h}$

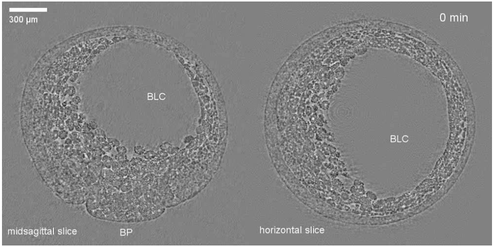

Xenopus gastrulation:
2-BM@APS
energy $\mathrm{E} = 30\,\mathrm{keV}$,
object-detector dist. z=62 cm
pixel size Δx=1 µm
bandwidth $\Delta \mathrm{E}/\mathrm{E}=10^{-2}$
exposure time/image Δt=15 ms
time lapse $\sim 2\,\mathrm{h}$

[Moosmann et al., Nature; Moosmann et al., Nature Protocols; Nawy, Nature Methods (research highlight)]

Digital study

Using dense & deep 3D information allows to digitally study

- Structural changes, gene expression, perturbation experiments: signal transduction and functioning of gene regulatory networks
- Cell and tissue dynamics: exchange of fluids and nutrients, deeply buried transient structures, cell migratory behaviour, ...
- Propulsion mechanisms for cell and tissue migration: differential flow-field analysis (convergent extension, cell-cell adhesion, cell-matrix interaction, ...)

Experimental setup

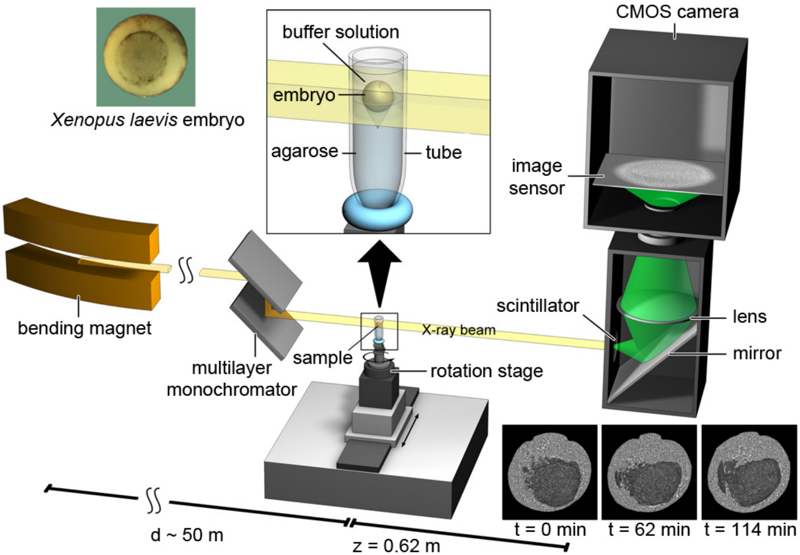

Propagation-based phase contrast

- Simple setup: no additional optics, no scanning, no stepping $\rightarrow$ stable, fast, efficient
- Intensity contrast emerges via free-space propagation of transmitted wave field

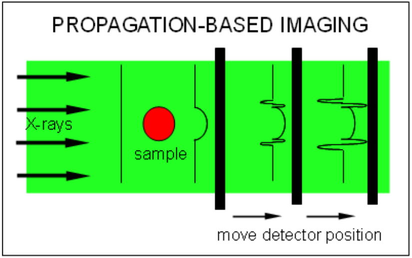

Sequence of intensity maps I_z: signal increases

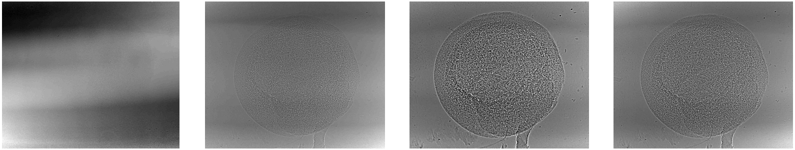

0.5 cm 18 cm 58 cm 108 cm

object-detector distance z

Phase contrast

- Rewrite Fresnel diffraction integral [Guigay 1977]

$$\mathcal{F}I_z(\boldsymbol{\xi}) = \int \mathrm{d}\boldsymbol{x} \, \exp\left(-i2\pi \boldsymbol{x} \cdot \boldsymbol{\xi}\right) \Psi_0 \left(\boldsymbol{x} - \tfrac{\lambda z}{2} \boldsymbol{\xi}\right) \Psi_0^* \left(\boldsymbol{x} + \tfrac{\lambda z}{2} \boldsymbol{\xi}\right)$$

$$\boldsymbol{x}, \boldsymbol{\xi} \in \mathbb{R}^2$$

- Intensity contrast $g_z = I_z / I_0 - 1$
- Expand exponential of exit wave field $\Psi_0 = \sqrt{I_0} \exp\left(i\phi_0\right)$
- Guigay up to $\mathcal{O}(\phi_0)$ (pure-phase object)

$$\begin{aligned}
\mathcal{F}g_z(\boldsymbol{\xi}) &= 2 \sin(\pi \lambda z \boldsymbol{\xi}^2) \mathcal{F}\phi_0(\boldsymbol{\xi}) \\
&- \cos(\pi \lambda z \boldsymbol{\xi}^2) \int \mathrm{d}\boldsymbol{\xi}' \, \mathcal{F}\phi_0(\boldsymbol{\xi}') \, \mathcal{F}\phi_0(\boldsymbol{\xi} - \boldsymbol{\xi}') \\
&+ \exp\left(i\pi \lambda z \boldsymbol{\xi}^2\right) \int \mathrm{d}\boldsymbol{\xi}' \, \exp\left(-i2\pi \lambda z \boldsymbol{\xi} \cdot \boldsymbol{\xi}'\right) \mathcal{F}\phi_0(\boldsymbol{\xi}') \, \mathcal{F}\phi_0(\boldsymbol{\xi} - \boldsymbol{\xi}')
\end{aligned}$$

Phase retrieval

Linear models

- Contrast transfer function (CTF)
  - Small relative phase variations:
    $\left|\phi_0(\boldsymbol{x} + \frac{\lambda z}{2}\boldsymbol{\xi}) - \phi_0(\boldsymbol{x} - \frac{\lambda z}{2}\boldsymbol{\xi})\right| \ll 1$
  - High resolution

$$\mathcal{F}\phi_0(\boldsymbol{\xi}) = \frac{\mathcal{F}g_z(\boldsymbol{\xi})}{2\sin(\pi\lambda z\boldsymbol{\xi}^2)}$$

[Guigay 1977; Gureyev et al. 2006; Cloetens 1998]

- Paganin phase retrieval
  - Edge-enhancement regime:
    small propagation distance
  - Low-pass filter
  - Robust

$$\mathcal{F}\phi_0(\boldsymbol{\xi}) = \frac{\mathcal{F}g_z(\boldsymbol{\xi})}{2\pi\lambda z\boldsymbol{\xi}^2}$$

[Teague 1982; Paganin & Nugent 1998; Bronnikov 2003]

Evolution of contrast transfer

- Compute intensity contrast from input phase map (Lena test pattern)
- Amplify phase variations by upscaling of input phase
- Consider Fourier transformed intensity (contrast transfer) as a function of distance

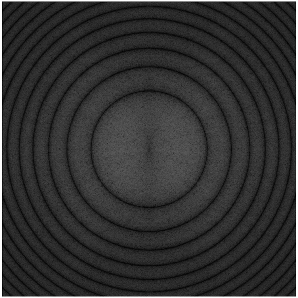

$|\mathcal{F}I_z|\,(\boldsymbol{\xi})$

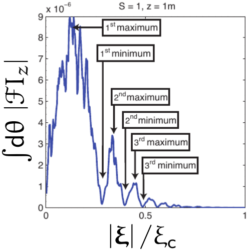

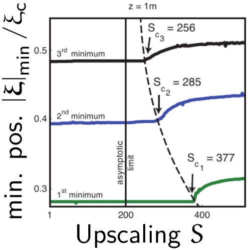

Phase retrieval: quasiparticle approach

- Fourier space filter: crop regions around minima
- Phase retrieval via CTF using filtered intensity

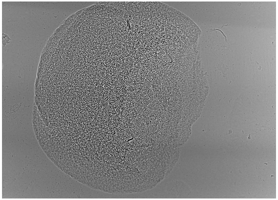

I_z

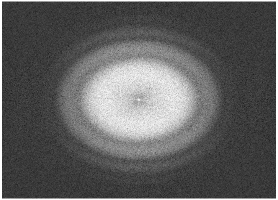

$|\mathcal{F}\mathrm{I}_z|$

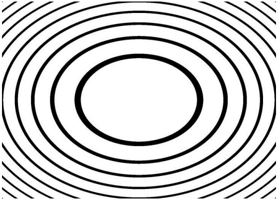

binary filter

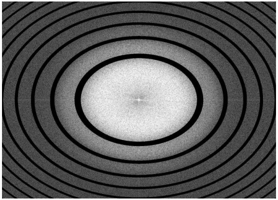

filtered $|\mathcal{F}\mathrm{I}_z|$

Data: TopoTomo@ANKA

Tomography: Paganin vs CTF vs QP

Xenopus, 4-cell stage, ID19@ESRF, $E = 20\,\mathrm{keV}$, $\Delta E/E = 10^{-4}$, $z = 1\,\mathrm{m}$, $\Delta x = 0.75\,\mu\mathrm{m}$

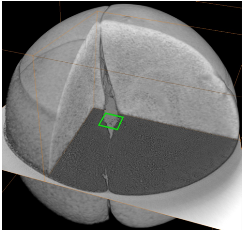
Rendering

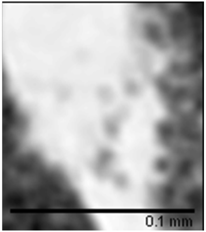

Paganin

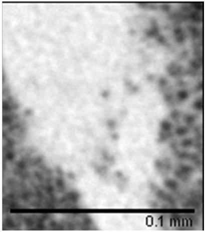

Quasiparticle

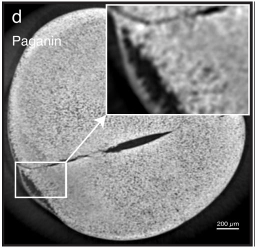

Paganin

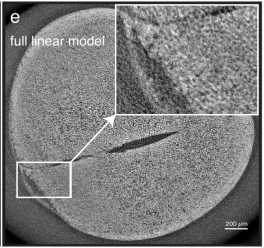

CTF

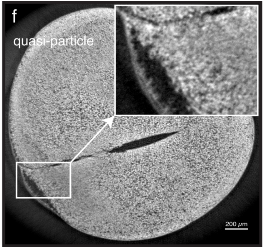

Quasiparticle

In vivo imaging: Considerations

- Motion blurring due to cell movement: $\sim 4\,\mu\text{m}$
  - Acquisition time for tomogram at resolution: $\lesssim 30\,\text{s}$
  - Required flux density: $> 10^{12}$ photons/s/mm^2
- Dose effects: heat load, double-strand breaking, radiolysis of water $\rightarrow$ free radicals
- Setup optimisation
  - Energy: dose vs photon flux vs phase contrast vs detection efficiency
  - Exposure time: dose vs signal-to-noise vs motion blurring
  - Object-detector distance: signal-to-noise vs blurring (finite source size, coherence, nonlinear propagation effects)
  - Tomography: number of projection, fast shutter influencing dose, resolution, rotation blurring, ...

4D in vivo tomography

Xenopus gastrulation:
2-BM@APS, time lapse: 2 h,
time between tomograms:
10 min, $\Delta x = 1\,\mu m$, $E = 30\,keV$,
$\Delta E/E = 10^{-2}$

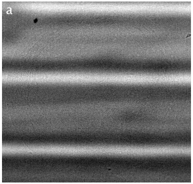

raw projection

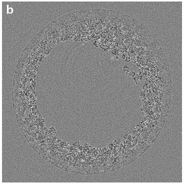

intensity

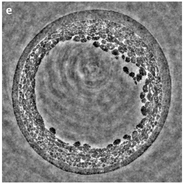

phase

tomographic reconstruction

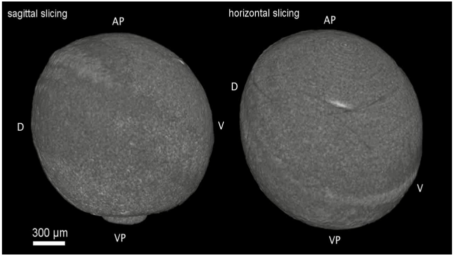

Slicing through rendered volume

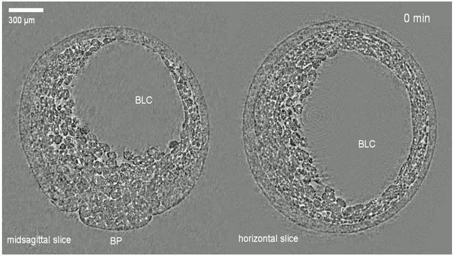

Time-lapse of reconstructed central slice

New observation: transient structure

- Confrontation of head & ventral mesendoderm: formation of a transient ridge
- Not observable in fixed embryos or implants

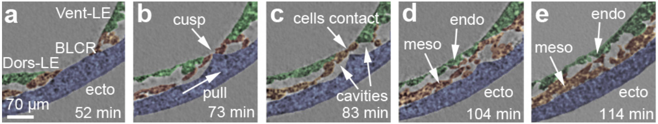

Time lapse of reconstructed slice

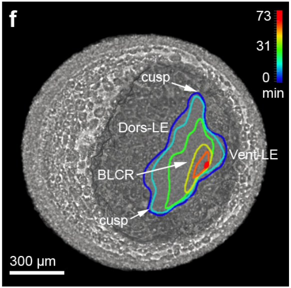

Moving contour of leading-edge mesendoderm

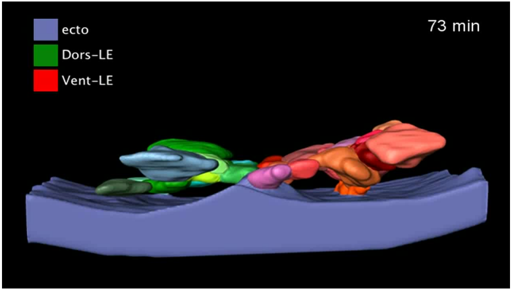

Segmented structures

Data analysis

- Visual inspection

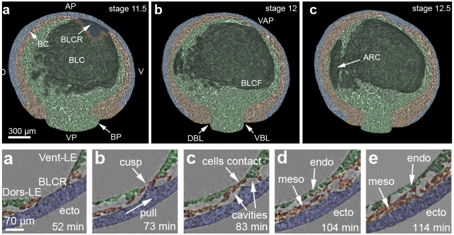

- Segmentation

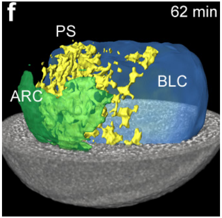

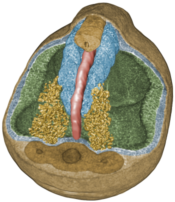

- Optical flow: overall dynamics
- Differential flow: collective vs individual movement
- Integrated flow: cell tracking

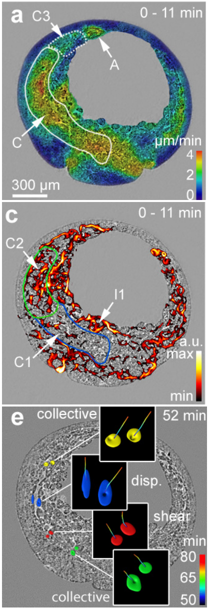

Thank you for your attention!

Segmentation & volume analysis

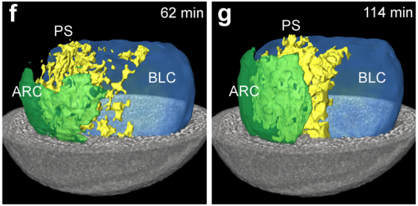

Archenteron inflation

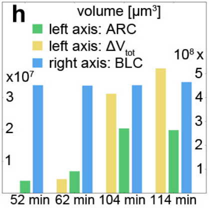

Volume balancing

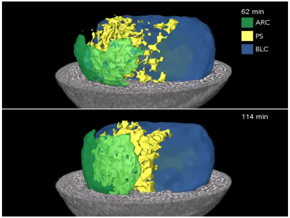

Segmented cavities

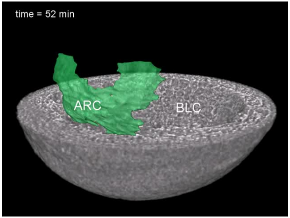

Inflating archenteron

- Conclusion: Archenteron inflation is driven by uptake of external water

Optical flow

- Visualising overall dynamics

Rendering of halved embryo

Velocity field on central slab

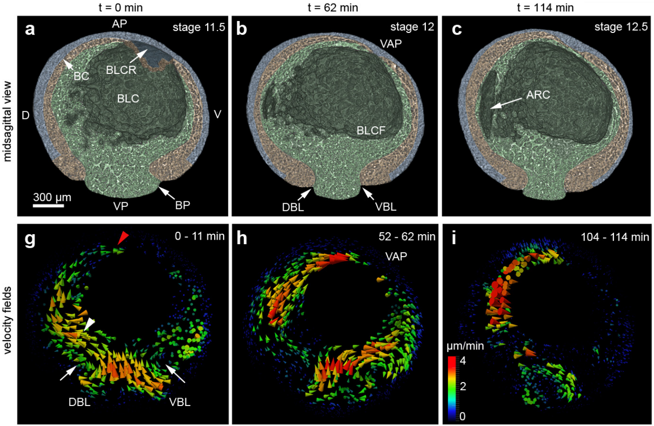

Differential optical flow

- Collective vs individual movement
- Propulsion mechanisms

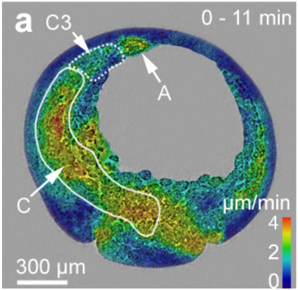

Magnitude of flow field

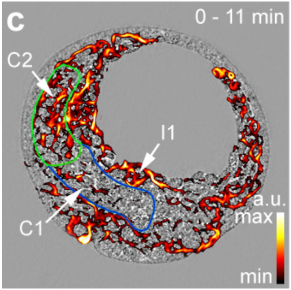

Magnitude of differential flow field

Integrated optical flow

- Cell tracking via time integration

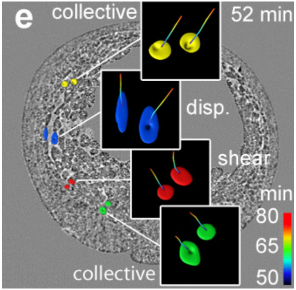

Trajectories of cell pairs

Outlook

- 4th generation synchrotron upgrades implementing multi-bend achromat lattices: drastically enhanced coherence $\rightarrow$ enhanced contrast, allows larger z
- Cone-beam magnification using Kirkpatrick Baez mirrors, ...
- Optimising detector system: scintillator, microscope, camera, blurring, deconvolution, point spread function, ...
- Tomography: fast shutter, dose, noise, stepping vs on-the-fly, alternative reconstruction techniques: algebraic, iterative, neural networks, sparsity, dictionary learning, ...
- Combination of X-ray phase-contrast & confocal fluorescence microscopy
- Systematic dose studies: dose delay effects, use of radical scavengers, find phenomenological function describing dose expression effects, ...
- Upcoming experiments: emigration & delamination processes of neural crest cells as a model for on-set of cancer metastasis
- Perturbation experiments (wildtype vs morphant embyros): role of adhesion molecules, signalling pathways, transcription